Published as: *Nat Genet*. 2014 June ; 46(6): 613–617.

Recurrent activating mutation in *PRKACA* in cortisol-producing adrenal tumors

Gerald Goh[1,2], **Ute I. Scholl**[1,2,3], **James M. Healy**[4], **Murim Choi**[1,2,5], **Manju L. Prasad**[6], **Carol Nelson-Williams**[1,2], **John W. Kuntsman**[4], **Reju Korah**[4], **Anna-Carinna Suttorp**[7], **Dimo Dietrich**[8], **Matthias Haase**[9], **Holger S. Willenberg**[9], **Peter Stålberg**[10], **Per Hellman**[10], **Göran Åkerström**[10], **Peyman Björklund**[10], **Tobias Carling**[4,11], and **Richard P. Lifton**[1,2,5]

[1]Department of Genetics, Yale University School of Medicine, New Haven, CT 06510, USA

[2]Howard Hughes Medical Institute, Yale University School of Medicine, New Haven, CT 06510, USA

[3]Division of Nephrology, University Hospital Düsseldorf, Düsseldorf, Germany

[4]Department of Surgery, Yale Endocrine Neoplasia Laboratory, Yale University School of Medicine, New Haven, CT 06510, USA

[5]Yale Center for Mendelian Genomics, New Haven, CT 06510, USA

[6]Department of Pathology, Yale University School of Medicine, New Haven, CT 06510, USA

[7]Department of Pathology, University Hospital Düsseldorf, Düsseldorf, Germany

[8]Institute of Pathology, University of Bonn, Bonn, Germany

[9]Division of Endocrinology and Diabetology, University Hospital Düsseldorf, Düsseldorf, Germany

[10]Department of Surgical Sciences, Uppsala University, Uppsala, Sweden

[11]Yale Cancer Center, Yale University School of Medicine, New Haven, CT 06510, USA

Abstract

Adrenal tumors autonomously producing cortisol cause Cushing syndrome[1–4]. Exome sequencing of 25 tumor-normal pairs revealed two groups. Eight tumors (including 3 carcinomas) had many

Correspondence to: Richard P. Lifton, M.D., Ph.D., Departments of Genetics and Internal Medicine, Howard Hughes Medical Institute, Yale University School of Medicine, 333 Cedar St., SHM I308, New Haven, CT 06510, USA. Telephone: +1-203-737-4420, Fax: +1-203-785-7560, richard.lifton@yale.edu.

Accession numbers.
Somatic mutations found by exome sequencing have been deposited in ClinVar under the batch accession 24068. RNA-seq data generated has been deposited in GEO.

The authors declare no competing financial interests.

Author contributions
UIS, JMH, MLP, JWK, RK, ACS, DD, MH, HSW, PS, PH, PB, GA and TC ascertained and recruited patients, obtained samples and medical records; UIS, RK, PB and CNW prepared DNA and RNA samples and maintained sample archives; GG performed and analyzed targeted DNA and RNA sequencing; GG, MC and RPL analyzed exome sequencing and RNA sequencing results; GG made constructs and performed immunoprecipitation and western blot analysis; GG and JMH performed immunohistochemistry; GG and MLP reviewed histology and immunohistochemistry; GG, UIS and RPL wrote the manuscript.

somatic copy number variants (CNV+) with frequent deletion of *CDC42* and *CDKN2A*, amplification of 5q31.2, and protein-altering mutations in *TP53* and *RB1*. Seventeen (all adenomas) had no CNVs (CNV-), *TP53* or *RB1* mutations. Six of these had known gain of function mutations in *CTNNB1*[5,6] (beta-catenin) or *GNAS*[7,8] ($G\alpha_s$), Six others had somatic p.Leu206Arg mutations in *PRKACA* (protein kinase A (PKA) catalytic subunit). Further sequencing identified this mutation in 13 of 63 tumors (35% of adenomas with overt CS). *PRKACA*, *GNAS* and *CTNNB1* mutations were mutually exclusive. Leu206 directly interacts with PKA's regulatory subunit, PRKAR1A[9,10]. $PRKACA^{L206R}$ loses PRKAR1A binding, increasing phosphorylation of downstream targets. PKA activity induces cortisol production and cell proliferation[11–15], providing a mechanism for tumor development. These findings define distinct mechanisms underlying adrenal cortisol-producing tumors.

Cortisol production is normally tightly regulated. Stress signals lead to hypothalamic release of corticotropin releasing hormone (CRH) and vasopressin, inducing pituitary secretion of adrenocorticotropic hormone (ACTH), which binds its G-protein coupled receptor (melanocortin receptor 2) in adrenal fasciculata, activating adenylate cyclase[16–19]. The resulting cAMP binds the regulatory subunit of PKA, inducing release of the PKA catalytic subunit, allowing phosphorylation of downstream targets such as CREB[20,21]. This induces cortisol biosynthesis and cell proliferation[21–23].

Cushing syndrome (CS) results from excessive cortisol production, causing metabolic abnormalities including central obesity, myopathy, diabetes, hypertension and osteoporosis[2,24]. This arises from tumors that constitutively produce CRH or ACTH, or from adrenal tumors that autonomously produce cortisol[1]. Somatic activating mutations in *CTNNB1* (beta-catenin) or *GNAS* (encoding $G\alpha_s$, which activates adenylate cyclase) have been found in a subset of these adrenal tumors[5–8]. Additionally, germline or mosaic mutations in *GNAS*, *PRKAR1A* (encoding the regulatory subunit of PKA), or cAMP phosphodiesterases (*PDE11A* or *PDE8B*) cause increased cAMP signaling and syndromes that include CS typically with adrenal hyperplasia.[11–13,15,25–27]. Thus, increased cAMP signaling in adrenal fasciculata is sufficient to increase cortisol production and adrenal cell mass.

Nonetheless, the pathogenesis of the vast majority of autonomous cortisol-producing adrenal tumors is unknown. We initially studied 25 patients diagnosed with autonomous cortisol-producing tumors. The diagnosis was based on elevated 24-hour urinary cortisol with suppressed ACTH level and/or pathological (i.e. non-suppressed) dexamethasone suppression test, and an adrenal tumor[28]. Eleven subjects had clinical stigmata of CS (Methods, Supplementary Table 1). Surgical pathology revealed tumors of mean size of 5.2 cm; 22 tumors were classified as adrenocortical adenomas (ACA) and 3 as adrenocortical carcinomas (ACC).

Exome sequencing on tumor and matched normal DNA was performed. 90% of the targeted bases in tumors had 20 or more independent reads (Supplementary Table 2). Mean tumor purity was estimated at 38%, and somatic single nucleotide variants (SNVs) and somatic copy number variants (CNVs) were called (see Methods). Mutations of interest were validated by direct Sanger sequencing.

The results identified two distinct groups of tumors with qualitative differences CNV number. Eight tumors (CNV+, including all three carcinomas) had 13.4 ± 3.9 CNVs (range 7–18, Supplementary Fig. 1) while 17 (CNV−) had zero. CNV+ tumors had a higher somatic SNV mutation rate (8.0×10^{-7} vs. 2.8×10^{-7}; $P = 1.3 \times 10^{-3}$, Mann-Whitney U test) and more protein-altering somatic mutations per tumor (16.1 vs. 5.6; $P = 8 \times 10^{-4}$, Mann-Whitney U test; Fig. 1a). These differences remained significant when carcinomas were removed from analysis (mutation rate 5.4×10^{-7}, $P = 0.02$; protein-altering mutations 10.4, $P = 0$ .01).

CNV+ tumors had significant focal losses of 3 chromosome segments (GISTIC[29] q-value < 0.25; Supplementary Fig. 2). Deletions of 1p36.12 and 9p21.3 included cancer-related genes *CDC42* and *CDKN2A*, respectively; 10p12.33 deletion contained *miR-511*, which shows reduced expression in ACCs[30]. A focal gain at 5q31.2 (q-value = 0.16) included *WNT8a*. Wnt signaling is a proliferative signal in adrenal cortex[5], and gain of function mutations in beta-catenin are common in adrenal tumors[31]. Two CNV+ tumors had known activating mutations in *CTNNB1* (Supplementary Table 3).

CNV+ tumors also had somatic mutations in cancer-related genes *TP53* and *RB1*, in all cases in segments with loss of heterozygosity (LOH; Fig. 1c). Mutations in these genes were not found in CNV− tumors ($P = 5.5 \times 10^{-3}$, Fisher's exact test). LOH at *TP53* in all cases resulted from loss of one copy of the entire chromosome 17 (Supplementary Fig. 1); TP53-associated cancers such as colon, lung and breast typically have deletion confined to 17p[32–35]. Interestingly, 17q includes *PRKAR1A* raising the question of whether heterozygous deletion of PRKAR1A might contribute to cortisol excess in these tumors. No other genes were significantly mutated (Supplementary Table 3). Tumors clinically classified as adenomas in the CNV+ group all had Weiss scores of 0 or 1, and, where studied, low Ki67 staining (Supplementary Table 1), providing no histologic evidence of carcinoma.

The remaining 17 tumors had a mean of only 1.6 silent and 5.6 protein-altering mutations (Fig. 1a). Known gain of function somatic mutations[31,36]. were found in *CTNNB1* (four tumors; p.Ser45Pro, p.Asp32Gly) or *GNAS* (two tumors; p.Arg201His, p.Gln227Glu) (Supplementary Table 3).

Additionally, the identical somatic A>C mutation in *PRKACA* (encoding the alpha isoform of the catalytic subunit of cAMP-dependent protein kinase A), resulting in a p.Leu206Arg (NM_002730.3:c.617A>C) substitution (Fig. 2a, Supplementary Table 4), was found in 6 CNV-tumors. This mutation has not been previously reported (absent from >10,000 exomes in public and Yale databases, and the Catalogue of somatic mutations in cancer, COSMIC). The read counts in all cases were consistent with heterozygous somatic mutations. These mutations were mutually exclusive with *CTNNB1* and *GNAS* mutations (Fig. 1c, $P = 0.043$, Fisher's exact test). Both wildtype (WT) and mutant *PRKACA* transcripts were detected in tumor cDNA (Supplementary Fig. 3). No other genes were mutated in more than one tumor.

Segments of *PRKACA*, *GNAS* and *CTNNB1* harboring gain of function mutations were amplified by PCR of DNA from 31 additional cortisol-producing adrenal tumors and

matched germline samples (available for 20 subjects) followed by Sanger sequencing (Supplementary Table 1). Seven additional tumors without matched normal DNA had exome sequencing. These comprised 33 ACAs and 5 ACCs. The *PRKACA* p.Leu206Arg mutation was identified in 7 additional tumors, collectively in 13 of 63 tumors (21%; 24% of all ACAs; 35% of ACAs associated with overt CS). The probability of finding the identical somatic mutation at any base in the exome 13 or more times by chance in 63 tumors is $< 10^{-62}$ (Binomial test). Activating *CTNNB1* and *GNAS* mutations were found in a total of 10 (15.9%), and 3 tumors (4.8%), respectively. *PRKACA, CTNNB1* and *GNAS* mutations remained mutually exclusive ($P = 0.02$, Monte Carlo simulation).

PRKACA is the most highly expressed catalytic isoform in human adrenal (Supplementary Table 5); the most highly expressed regulatory subunit is *PRKAR1A*. PRKACA phosphorylates the R-R-X-S/T-Φ motif (Φ is hydrophobic)[37]. The regulatory subunit binds to PRKACA catalytic cleft via a pseudosubstrate sequence R-R-G-A-I[9]; the isoleucine of PRKAR1A fits in a hydrophobic cleft in the catalytic domain formed by Leu206 and Leu199[38,39] (Fig. 2c, 2d[10]). Leu206 is conserved in orthologs from invertebrates to humans, while yeast has the isomer Ile (Fig. 2b). The p.Leu206Arg substitution is likely to disrupt this interaction (Fig. 2e, 2f), resulting in constitutive PKA activity.

We expressed PRKAR1A and either $PRKACA^{WT}$ or $PRKACA^{L206R}$ (both with C-terminal FLAG epitope tag), in equimolar ratios in HEK293T cells. PRKAR1A shows low endogenous levels that are increased by transfection (Fig. 3a). Cell lysates were immunoprecipitated (IP) with anti-FLAG to pull down PRKACA, followed by Western blotting using anti-PRKAR1A antibodies. In 3 independent transfections, immunoprecipitation with $PRKACA^{WT}$ robustly pulled down PRKAR1A, while no PRKAR1A was detected after IP with $PRKACA^{L206R}$ (Fig. 3a).

Unbound $PRKACA^{L206R}$ should result in increased phosphorylation at targets such as Ser133 of CREB ($CREB^{Ser133\text{-}P}$). Western blotting of lysates from cells expressing wildtype or mutant PRKACA and PRKAR1A with an antibody specific for phospho-Ser133 demonstrated that $PRKACA^{L206R}$ produced ~4-fold increased $CREB^{Ser133\text{-}P}$ versus $PRKACA^{WT}$ ($P = 0.037$, T-test; Fig. 3b). Similarly increased phosphorylation was seen at Ser63 in ATF1, another PKA target ($P= 0.002$, T-test; Fig. 3b). Immunohistochemistry for $CREB^{Ser133\text{-}P}$ showed increased staining in eight *PRKACA*-mutant tumors compared to 5 adenomas without *PRKACA, GNAS* or *CTNNB1* mutations (median 55% versus 10%, Supplementary Fig. 4, Supplementary Table 6). Additional histologic features are described in Supplementary Fig. 5.

Adenomas with *PRKACA* or *GNAS* mutations were significantly smaller than adenomas without (28.7 ± 7.3 mm versus 39.2 ± 15.9 mm, s.d.; $P = 0.035$, Mann-Whitney U test) and patients presented at significantly younger ages (45.3 ± 13.5 versus 52.5 ± 11.9 years, s.d.; $P = 0.045$, Mann-Whitney U test). They were also significantly associated with overt CS (13/16 with *PRKACA* or *GNAS* mutation with overt CS, versus 16/39 without, $P = 0.008$, Fisher's exact test).

These results implicate a recurrent gain-of-function mutation in *PRKACA* in cortisol-producing adrenal adenomas. This was the most frequently mutated gene in our cohort. Mutant PRKACA has drastically diminished binding to its regulatory subunit, leading to increased PKA enzymatic activity.

Because of strong prior evidence that increased cAMP signaling is sufficient for cell proliferation and cortisol production[7,40–42], these *PRKACA* mutations are likely sufficient for tumor formation (Supplementary Fig. 6). The absence of other mutations likely to contribute to neoplasia supports this notion. The same applies to activating *GNAS* mutations. These findings are analogous to observations in adrenal aldosterone-producing adenomas, in which the single mutations are sufficient for cell proliferation and hormone production[43–45]. In both diseases, the coupling of signaling pathways to both hormone production and cell proliferation provides a mechanism for increasing the mass of hormone-producing cells when demand for hormone is high. These observations suggest that PKA inhibitors could be of benefit in controlling tumor growth and hormone production in tumors bearing this mutation.

Mutations in *PRKACA*, *GNAS* and *CTNNB1* were found in 12 of 17 CNV− tumors. The pathogenesis of the remaining five tumors without known drivers remains unknown, leaving open the question of whether they might result from mutations outside the coding region.

The mutual exclusivity of *PRKACA*, *GNAS* and *CTNNB1* mutations suggests they phenocopy one another. Previous studies have found that increased cAMP signaling increased Wnt/beta-catenin signaling[46,47]; similarly, PKA can phosphorylate beta-catenin, inhibiting ubiquitination and increasing signaling[48,49]. Wnt signaling promotes proliferation of adrenal fasciculata cells, and there is evidence for a role in activation of the steroid biosynthetic pathway[50]. Nonetheless, activating *CTNNB1* mutations are also found in non-hormone producing adrenocortical tumors and other cancers[31,51,52]. Further work will be required to establish the factors that determine which tumors with *CTNNB1* mutations autonomously produce hormones.

While this paper was in review, this same somatic PRKACA mutation was reported in 37% of adrenal adenomas associated with overt Cushing syndrome and 22% of all cortisol-producing adenomas from an independent cohort. Use of a cell-based FRET assay for PKA activity provided evidence of constitutive activity of the mutant protein[53].

The striking differences in mutation spectrum between CNV+ and CNV− tumors suggest two distinct mechanisms for these tumors. Interestingly, the somatic mutation spectrum of CNV+ tumors diagnosed by rigorous histologic criteria as adenomas was more similar to that of CNV+ carcinomas and other cancers than CNV− adenomas. Larger cortisol-producing adrenal tumors are believed to make cortisol inefficiently owing to lack of activation of the cortisol biosynthetic pathway, while smaller tumors are more efficient due to induction of cortisol biosynthetic enzymes[54]. The current findings support this observation, because smaller tumors more frequently have *PRKACA* and *GNAS* mutations, activating the cAMP signaling pathway.

The mutation spectrum in CNV+ adenomas suggests they may have greater malignant potential. These tumors may come to early attention due to clinical signs and symptoms of cortisol excess. Interestingly, some adrenal cortisol-producing tumors initially classified as benign have recurred with invasive or metastatic disease[55]. Similarly, other studies in mice and humans have also suggested a multistep model of progression from adrenal hyperplasia to adenoma and carcinoma[56–58]. These observations suggest that CNV+ adenomas might warrant closer clinical follow-up.

While all tumors in our study were diagnosed as having autonomous cortisol production by experienced endocrinologists and surgeons in tertiary referral hospitals, supporting data for 9 patients referred from outside hospitals had incomplete documentation in available medical records (Supplementary Table 1). Exclusion of these tumors (14% of the total) did not significantly alter the conclusions. These 9 tumors comprised 3 carcinomas and 6 adenomas with no mutation in *PRKACA* or *GNAS*, and 1 with *CTNNB1* mutation.

Lastly, activating *GNAS* mutations are found in growth-hormone secreting pituitary tumors and thyroid adenomas[59]. The finding that *PRKACA* mutation can phenocopy activating *GNAS* mutations in adrenal tumors raises the possibility that mutations in *PRKACA* or other genes that increase cAMP signaling might be found in these other tumors as well.

Online Methods

Patients and specimens

Matched fresh-frozen cortisol-producing adrenocortical tumors and either venous blood samples or adjacent normal tissue were obtained from patients undergoing adrenalectomy at Yale New Haven Hospital, Uppsala University Hospital. Additional tumors and matched normal samples were obtained from formalin-fixed paraffin-embedded samples in Yale Department of Pathology, University of Bonn and University of Düsseldorf. The research protocols of all studies were approved by local IRBs.

All tumors included in this study were determined by experienced endocrinologists and endocrine surgeons at tertiary referral hospitals to have ACTH-independent cortisol production, resulting in either subclinical or overt Cushing syndrome at the time of surgery, with surgical pathology consistent with that diagnosis. Patient demographics, tumor characteristics, laboratory test results and clinical features are summarized in Supplementary Table 1. Some clinical records were incomplete owing to evaluation having been performed at outside hospitals, with detailed records missing from the tertiary hospital medical record.

Tumors were classified by an endocrine pathologist blinded to genotypes; tumor histology was categorized by gross assessment of tumor, percentage of oncocytic cells, and nuclear atypia graded from unremarkable to severe atypia. Weiss scores[60,61] were determined for each tumor, and proliferative index using Ki-67 (clone MIB-1, Dakopatts, dil 1:300, Epitope retrieval: high pH for 20′ Leica Bond III) was performed in tumors on the judgment of the pathologist. Nuclear staining in tumor cells was assessed as positive, and a percentage was calculated after assessing 4000 to 5000 tumor cell nuclei (10 high power fields).

DNA and RNA were isolated from non-FFPE samples using the Allprep kit (Qiagen) following manufacturer's instructions. For FFPE samples, DNA was prepared with the BiOstic FFPE Tissue DNA Isolation kit (MO BIO Laboratories) using a modified protocol.

Whole exome sequencing and analysis

Targeted capture was performed using the NimbleGen 2.1 Exome reagent followed by sequencing on the Illumina platform as previously described[44]. Sequences were aligned to NCBI Build 36 of the human genome using the ELAND program (Illumina). Somatic mutations were called based on the significance of differences in reference and non-reference read distributions between tumor and matched normal samples. Calls were further evaluated by manual inspection of read alignments.

The somatic mutation rate and estimations of tumor purity were calculated as previously described[44]. MutSig[62] was used to determine if genes were mutated more often than expected by chance. CNVs were identified by comparing coverage depth ratios of tumor and matched normal samples after normalizing for mean coverage depth of each exome, and changes in minor allele frequency at informative SNPs. GISTIC2.0 was used to assess the significance of recurrent CNVs as described previously[29].

Sanger sequencing of genomic DNA

Direct bidirectional Sanger sequencing of *PRKACA* Leu206, exon 3 of *CTNNB1* and *GNAS* (Arg201 and Gln227) from genomic DNA from tumors and matched normal samples was performed following PCR amplification using specific primers. Primer sequences are listed in Supplementary Table 7.

Whole transcriptome (mRNA-Seq) profiling

Ribosomal RNA (rRNA) was removed from total RNA using the Ribo-Zero rRNA Removal Kit (Epicenter) according to manufacturer's instructions. cDNA was synthesized and libraries prepared using the Illumina RNA-Seq kit, followed by sequencing on Illumina HiSeq instrument. RNAseq data for normal adrenal gland was obtained from the Illumina Human Body Map 2.0 Project[63]. Sequences were aligned using TopHat version 2.08 and assembled into transcripts using Cufflinks version 2.0.2[64,65].

Clones and mutagenesis

Expression plasmids encoding human PRKACA and PRKAR1A were obtained from Origene (RC210332, NM_002730; RC203828, NM_002734). The Leu206Arg mutation was introduced into PRKACA using the QuikChange site-directed mutagenesis system (Stratagene), and validated by sequencing the complete coding region. Plasmids were prepared using the HiSpeed Plasmid Maxi Kit (Qiagen). The FLAG tag was deleted in the PRKAR1A construct for the IP experiment using EcoRV and PmeI restriction enzymes (New England Biolabs).

Transient transfection and IP

HEK293T cells (ECACC) were cultured in DMEM (Gibco) supplemented with 10% fetal bovine serum, penicillin (100 units/ml) and streptomycin (10mg/ml). Cells were transfected with expression plasmids using Lipofectamine 2000 (Life Technologies) according to manufacturer's instructions, followed by incubation for 48h. PRKACA and PRKAR1A were co-transfected at a molar ratio of 1:1. Cells were then washed in cold PBS and lysed at 4°C in lysis buffer as previously described[66]. Protein concentrations were quantified using a BCA Protein Assay Kit (Pierce), incubated with Anti-FLAG M2 Affinity gel (Sigma) at 4°C, washed and eluted with 3X FLAG peptide.

Western blotting

Protein extraction and Western Blotting were performed as previously described[66]. Lysates and immunoprecipitates were fractionated on 4–20% polyacrylamide gels, transferred to nitrocellulose membranes, and immunoblotted with primary antibodies: rabbit anti-FLAG (Sigma, 1:5,000), anti-CREB (CST, 1:1000), anti-Phospho-CREB (CST, 1:1000), anti-ATF1 (Millipore, 1:1000) or mouse anti-PRKAR1A (BD Biosciences, 1:500). Signals were visualized by chemiluminscence after incubation with peroxidase-conjugated secondary antibody.

Phospho-CREB staining

IHC was performed on slides from FFPE samples using a rabbit polyclonal antibody to Phospho-CREB (CST, 1:600). To determine specificity of antibody binding, blocking peptides specific to the antibody were used (CST). All slides were stripped of paraffin in xylene before rinsing in decreasing concentrations of ethanol, prior to antigen retrieval in boiling 10 mM Sodium Citrate + 0.05% Tween 20 at pH 6.0. Cells were permeabilized in 0.2% Triton X100 in PBS, then incubated in 3% hydrogen peroxide. Blocking was achieved with 10% BSA in PBS. After incubation with primary and secondary antibodies, slides were stained with DAB and counter-stained with Hematoxylin.

An experienced endocrine pathologist determined the percentage of nuclei stained positive for phosphorylated CREB by selecting most strongly staining area, and at least 100 nuclei were assessed for each tumor. Endothelial cells in the tumor were used as an internal positive control for regions where staining of tumor nuclei was not observed, and the presence of unstained nuclei was used as internal negative controls.

Statistical analysis

The data are summarized as means ± SEM. Two-tailed *t* tests, Mann-Whitney U tests and Fisher's exact tests were used for comparison between two groups. The *p* value for the probability of observed recurrent mutation occurring by chance was calculated as a binomial probability, using the somatic mutation rate of CNV− tumors.

Monte Carlo simulations (1×10^6 iterations) were performed to calculate the probability of observing mutually exclusive mutations in *PRKACA*, *CTNNB1* and *GNAS* by chance.

Supplementary Material

Refer to Web version on PubMed Central for supplementary material.

Acknowledgments

This work was supported in part by the US National Institutes of Health (NIH) Centers for Mendelian Genomics (5U54HG006504). GG is supported by the Agency for Science, Technology and Research, Singapore. TC is a Damon Runyon Clinical Investigator supported in part by the Damon Runyon Cancer Research Foundation. RPL is an Investigator of the Howard Hughes Medical Institute.

References

1. Hatipoglu BA. Cushing's syndrome. J Surg Oncol. 2012; 106:565–71. [PubMed: 22740318]
2. Orth DN. Cushing's syndrome. N Engl J Med. 1995; 332:791–803. [PubMed: 7862184]
3. Biller BM, et al. Treatment of adrenocorticotropin-dependent Cushing's syndrome: a consensus statement. J Clin Endocrinol Metab. 2008; 93:2454–62. [PubMed: 18413427]
4. Chiodini I. Clinical review: Diagnosis and treatment of subclinical hypercortisolism. J Clin Endocrinol Metab. 2011; 96:1223–36. [PubMed: 21367932]
5. El Wakil A, Lalli E. The Wnt/beta-catenin pathway in adrenocortical development and cancer. Mol Cell Endocrinol. 2011; 332:32–7. [PubMed: 21094679]
6. Tissier F, et al. Mutations of beta-catenin in adrenocortical tumors: activation of the Wnt signaling pathway is a frequent event in both benign and malignant adrenocortical tumors. Cancer Res. 2005; 65:7622–7. [PubMed: 16140927]
7. Almeida MQ, Stratakis CA. How does cAMP/protein kinase A signaling lead to tumors in the adrenal cortex and other tissues? Mol Cell Endocrinol. 2011; 336:162–8. [PubMed: 21111774]
8. Fragoso MC, et al. Cushing's syndrome secondary to adrenocorticotropin-independent macronodular adrenocortical hyperplasia due to activating mutations of GNAS1 gene. J Clin Endocrinol Metab. 2003; 88:2147–51. [PubMed: 12727968]
9. Kim C, Xuong NH, Taylor SS. Crystal structure of a complex between the catalytic and regulatory (RIalpha) subunits of PKA. Science. 2005; 307:690–6. [PubMed: 15692043]
10. Ubersax JA, Ferrell JE Jr. Mechanisms of specificity in protein phosphorylation. Nat Rev Mol Cell Biol. 2007; 8:530–41. [PubMed: 17585314]
11. Bertherat J, et al. Molecular and functional analysis of PRKAR1A and its locus (17q22-24) in sporadic adrenocortical tumors: 17q losses, somatic mutations, and protein kinase A expression and activity. Cancer Res. 2003; 63:5308–19. [PubMed: 14500362]
12. Casey M, et al. Mutations in the protein kinase A R1alpha regulatory subunit cause familial cardiac myxomas and Carney complex. J Clin Invest. 2000; 106:R31–8. [PubMed: 10974026]
13. Cazabat L, Ragazzon B, Groussin L, Bertherat J. PRKAR1A mutations in primary pigmented nodular adrenocortical disease. Pituitary. 2006; 9:211–9. [PubMed: 17036196]
14. Cho-Chung YS, Pepe S, Clair T, Budillon A, Nesterova M. cAMP-dependent protein kinase: role in normal and malignant growth. Crit Rev Oncol Hematol. 1995; 21:33–61. [PubMed: 8822496]
15. Kirschner LS, et al. Genetic heterogeneity and spectrum of mutations of the PRKAR1A gene in patients with the carney complex. Hum Mol Genet. 2000; 9:3037–46. [PubMed: 11115848]
16. Saffran M. Mechanisms of adrenocortical control. Br Med Bull. 1962; 18:122–6. [PubMed: 14495979]
17. Stocco DM, Clark BJ. Regulation of the acute production of steroids in steroidogenic cells. Endocr Rev. 1996; 17:221–44. [PubMed: 8771357]
18. Gillies GE, Linton EA, Lowry PJ. Corticotropin releasing activity of the new CRF is potentiated several times by vasopressin. Nature. 1982; 299:355–7. [PubMed: 6287293]
19. Rivier C, Vale W. Modulation of stress-induced ACTH release by corticotropin-releasing factor, catecholamines and vasopressin. Nature. 1983; 305:325–7. [PubMed: 6312319]

20. Ramachandran J, Tsubokawa M, Gohil K. Corticotropin receptors. Ann N Y Acad Sci. 1987; 512:415–25. [PubMed: 2831782]
21. Simpson ER, Waterman MR. Regulation of the synthesis of steroidogenic enzymes in adrenal cortical cells by ACTH. Annu Rev Physiol. 1988; 50:427–40. [PubMed: 2837136]
22. Roger PP, Reuse S, Maenhaut C, Dumont JE. Multiple facets of the modulation of growth by cAMP. Vitam Horm. 1995; 51:59–191. [PubMed: 7483330]
23. Rosenberg D, et al. Role of the PKA-regulated transcription factor CREB in development and tumorigenesis of endocrine tissues. Ann N Y Acad Sci. 2002; 968:65–74. [PubMed: 12119268]
24. Newell-Price J, Trainer P, Besser M, Grossman A. The diagnosis and differential diagnosis of Cushing's syndrome and pseudo-Cushing's states. Endocr Rev. 1998; 19:647–72. [PubMed: 9793762]
25. Almeida MQ, Stratakis CA. Carney complex and other conditions associated with micronodular adrenal hyperplasias. Best Pract Res Clin Endocrinol Metab. 2010; 24:907–14. [PubMed: 21115159]
26. Horvath A, et al. A genome-wide scan identifies mutations in the gene encoding phosphodiesterase 11A4 (PDE11A) in individuals with adrenocortical hyperplasia. Nat Genet. 2006; 38:794–800. [PubMed: 16767104]
27. Horvath A, et al. Adrenal hyperplasia and adenomas are associated with inhibition of phosphodiesterase 11A in carriers of PDE11A sequence variants that are frequent in the population. Cancer Res. 2006; 66:11571–5. [PubMed: 17178847]
28. Nieman LK, et al. The diagnosis of Cushing's syndrome: an Endocrine Society Clinical Practice Guideline. J Clin Endocrinol Metab. 2008; 93:1526–40. [PubMed: 18334580]
29. Mermel CH, et al. GISTIC2.0 facilitates sensitive and confident localization of the targets of focal somatic copy-number alteration in human cancers. Genome Biol. 2011; 12:R41. [PubMed: 21527027]
30. Tombol Z, et al. Integrative molecular bioinformatics study of human adrenocortical tumors: microRNA, tissue-specific target prediction, and pathway analysis. Endocr Relat Cancer. 2009; 16:895–906. [PubMed: 19546168]
31. Bonnet S, et al. Wnt/beta-catenin pathway activation in adrenocortical adenomas is frequently due to somatic CTNNB1-activating mutations, which are associated with larger and nonsecreting tumors: a study in cortisol-secreting and -nonsecreting tumors. J Clin Endocrinol Metab. 2011; 96:E419–26. [PubMed: 21084400]
32. Zhu J, et al. The UCSC Cancer Genomics Browser. Nat Methods. 2009; 6:239–40. [PubMed: 19333237]
33. Cancer Genome Atlas, N. Comprehensive molecular characterization of human colon and rectal cancer. Nature. 2012; 487:330–7. [PubMed: 22810696]
34. Cancer Genome Atlas, N. Comprehensive molecular portraits of human breast tumours. Nature. 2012; 490:61–70. [PubMed: 23000897]
35. Cancer Genome Atlas Research, N. Comprehensive genomic characterization of squamous cell lung cancers. Nature. 2012; 489:519–25. [PubMed: 22960745]
36. Hsiao HP, et al. Clinical and genetic heterogeneity, overlap with other tumor syndromes, and atypical glucocorticoid hormone secretion in adrenocorticotropin-independent macronodular adrenal hyperplasia compared with other adrenocortical tumors. J Clin Endocrinol Metab. 2009; 94:2930–7. [PubMed: 19509103]
37. Songyang Z, et al. Use of an oriented peptide library to determine the optimal substrates of protein kinases. Curr Biol. 1994; 4:973–82. [PubMed: 7874496]
38. Taylor SS, et al. Dynamics of signaling by PKA. Biochim Biophys Acta. 2005; 1754:25–37. [PubMed: 16214430]
39. Zheng J, et al. 2.2 A refined crystal structure of the catalytic subunit of cAMP-dependent protein kinase complexed with MnATP and a peptide inhibitor. Acta Crystallogr D Biol Crystallogr. 1993; 49:362–5. [PubMed: 15299527]
40. de Joussineau C, et al. The cAMP pathway and the control of adrenocortical development and growth. Mol Cell Endocrinol. 2012; 351:28–36. [PubMed: 22019902]

41. Lania AG, Mantovani G, Spada A. Mechanisms of disease: Mutations of G proteins and G-protein-coupled receptors in endocrine diseases. Nat Clin Pract Endocrinol Metab. 2006; 2:681–93. [PubMed: 17143315]
42. Meoli E, et al. Protein kinase A effects of an expressed PRKAR1A mutation associated with aggressive tumors. Cancer Res. 2008; 68:3133–41. [PubMed: 18451138]
43. Choi M, et al. K+ channel mutations in adrenal aldosterone-producing adenomas and hereditary hypertension. Science. 2011; 331:768–72. [PubMed: 21311022]
44. Scholl UI, et al. Somatic and germline CACNA1D calcium channel mutations in aldosterone-producing adenomas and primary aldosteronism. Nat Genet. 2013; 45:1050–4. [PubMed: 23913001]
45. Scholl UI, et al. Hypertension with or without adrenal hyperplasia due to different inherited mutations in the potassium channel KCNJ5. Proc Natl Acad Sci U S A. 2012; 109:2533–8. [PubMed: 22308486]
46. Almeida MQ, et al. Mouse Prkar1a haploinsufficiency leads to an increase in tumors in the Trp53+/− or Rb1+/− backgrounds and chemically induced skin papillomas by dysregulation of the cell cycle and Wnt signaling. Hum Mol Genet. 2010; 19:1387–98. [PubMed: 20080939]
47. Gaujoux S, et al. Wnt/beta-catenin and 3′,5′-cyclic adenosine 5′-monophosphate/protein kinase A signaling pathways alterations and somatic beta-catenin gene mutations in the progression of adrenocortical tumors. J Clin Endocrinol Metab. 2008; 93:4135–40. [PubMed: 18647815]
48. Hino S, Tanji C, Nakayama KI, Kikuchi A. Phosphorylation of beta-catenin by cyclic AMP-dependent protein kinase stabilizes beta-catenin through inhibition of its ubiquitination. Mol Cell Biol. 2005; 25:9063–72. [PubMed: 16199882]
49. Taurin S, Sandbo N, Qin Y, Browning D, Dulin NO. Phosphorylation of beta-catenin by cyclic AMP-dependent protein kinase. J Biol Chem. 2006; 281:9971–6. [PubMed: 16476742]
50. Schinner S, et al. Adipocyte-derived products induce the transcription of the StAR promoter and stimulate aldosterone and cortisol secretion from adrenocortical cells through the Wnt-signaling pathway. Int J Obes (Lond). 2007; 31:864–70. [PubMed: 17211444]
51. Cancer Genome Atlas Research, N. et al. Integrated genomic characterization of endometrial carcinoma. Nature. 2013; 497:67–73. [PubMed: 23636398]
52. Cleary SP, et al. Identification of driver genes in hepatocellular carcinoma by exome sequencing. Hepatology. 2013; 58:1693–1702. [PubMed: 23728943]
53. Beuschlein F, et al. Constitutive Activation of PKA Catalytic Subunit in Adrenal Cushing's Syndrome. N Engl J Med. 2014; 370:1019–1028. [PubMed: 24571724]
54. Zenkert S, et al. Steroidogenic acute regulatory protein mRNA expression in adrenal tumours. Eur J Endocrinol. 2000; 142:294–9. [PubMed: 10700725]
55. Brauckhoff M, et al. Peritoneal carcinosis in apparently benign cortisol producing adrenal adenoma >/= 5 cm in diameter: the need of regular postoperative surveillance. Exp Clin Endocrinol Diabetes. 2012; 120:472–6. [PubMed: 22851184]
56. Almeida MQ, et al. Integrated genomic analysis of nodular tissue in macronodular adrenocortical hyperplasia: progression of tumorigenesis in a disorder associated with multiple benign lesions. J Clin Endocrinol Metab. 2011; 96:E728–38. [PubMed: 21252250]
57. Heaton JH, et al. Progression to adrenocortical tumorigenesis in mice and humans through insulin-like growth factor 2 and beta-catenin. Am J Pathol. 2012; 181:1017–33. [PubMed: 22800756]
58. Ronchi CL, et al. Single nucleotide polymorphism array profiling of adrenocortical tumors--evidence for an adenoma carcinoma sequence? PLoS One. 2013; 8:e73959. [PubMed: 24066089]
59. Dhanasekaran N, Heasley LE, Johnson GL. G protein-coupled receptor systems involved in cell growth and oncogenesis. Endocr Rev. 1995; 16:259–70. [PubMed: 7671848]
60. Lau SK, Weiss LM. The Weiss system for evaluating adrenocortical neoplasms: 25 years later. Hum Pathol. 2009; 40:757–68. [PubMed: 19442788]
61. Duregon E, et al. Oncocytic adrenocortical tumors: diagnostic algorithm and mitochondrial DNA profile in 27 cases. Am J Surg Pathol. 2011; 35:1882–93. [PubMed: 21989346]
62. Lawrence MS, et al. Mutational heterogeneity in cancer and the search for new cancer-associated genes. Nature. 2013; 499:214–8. [PubMed: 23770567]

63. Farrell CM, et al. Current status and new features of the Consensus Coding Sequence database. Nucleic Acids Res. 2013

64. Kim D, et al. TopHat2: accurate alignment of transcriptomes in the presence of insertions, deletions and gene fusions. Genome Biol. 2013; 14:R36. [PubMed: 23618408]

65. Trapnell C, et al. Differential analysis of gene regulation at transcript resolution with RNA-seq. Nat Biotechnol. 2013; 31:46–53. [PubMed: 23222703]

66. Shibata S, Zhang J, Puthumana J, Stone KL, Lifton RP. Kelch-like 3 and Cullin 3 regulate electrolyte homeostasis via ubiquitination and degradation of WNK4. Proc Natl Acad Sci U S A. 2013; 110:7838–43. [PubMed: 23576762]

Figure 1.

Somatic mutations in cortisol-producing adrenal tumors. (**a**) The number of somatic mutations in each tumor is shown. Tumors are either adrenocortical carcinomas (ACC, in orange), CNV+ (in off-white) or CNV− (in white). (**b**) Recurrent copy number variants and GISTIC peaks identified in tumors. Likely driver genes are listed in parenthesis. Red, amplification; blue, deletion. (**c**) Somatic protein-altering mutations in genes frequently mutated in tumors. Each track describes presence (colored) or absence (off-white, white) of mutation in tumor for gene specified.

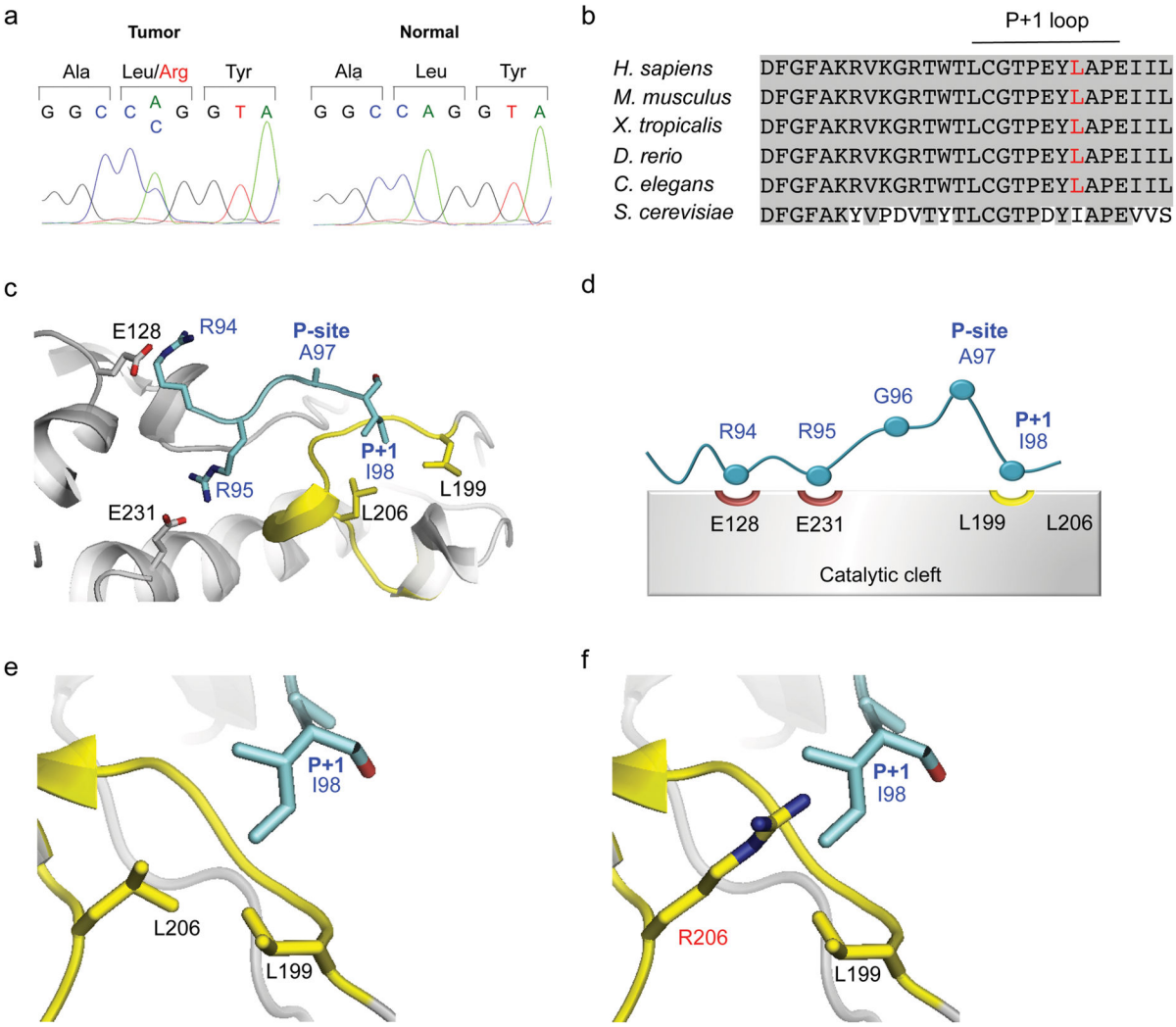

Figure 2.

PRKACA Leu206 interacts with PRKAR1A. (**a**) Representative chromatograms of Sanger DNA sequence of normal and tumor DNA for *PRKACA* codons 205–207; the tumor shows a heterozygous somatic p.Leu206Arg mutation. (**b**) Multiple sequence alignment of the activation loop of PRKACA. This segment is highly conserved from yeast to humans, with leucine at the position orthologous to Leu206 through invertebrates, and isoleucine in yeast. (**c**) Crystal structure of PRKACA and inhibitor (PDB: 1ATP)[9]. The inhibitory peptide (Arg^{94}-Arg-Asn-Ala-Ile^{98}) is shown in cyan while the P+1 loop of PRKACA is shown in yellow. Leu206 and Leu199 of PRKACA make van der Waals contacts with Ile98 of the inhibitory peptide, while arginines of the inhibitory peptide form salt bridges with glutamates of the catalytic cleft[10,38,39]. (**d**) Schematic illustration of the key interactions between the regulatory and catalytic subunit (adapted from ref. 10). (**e**) Close-up view of the interaction between Ile98 and Leu206, and (**f**) likely rotamer with Arg206 substitution.

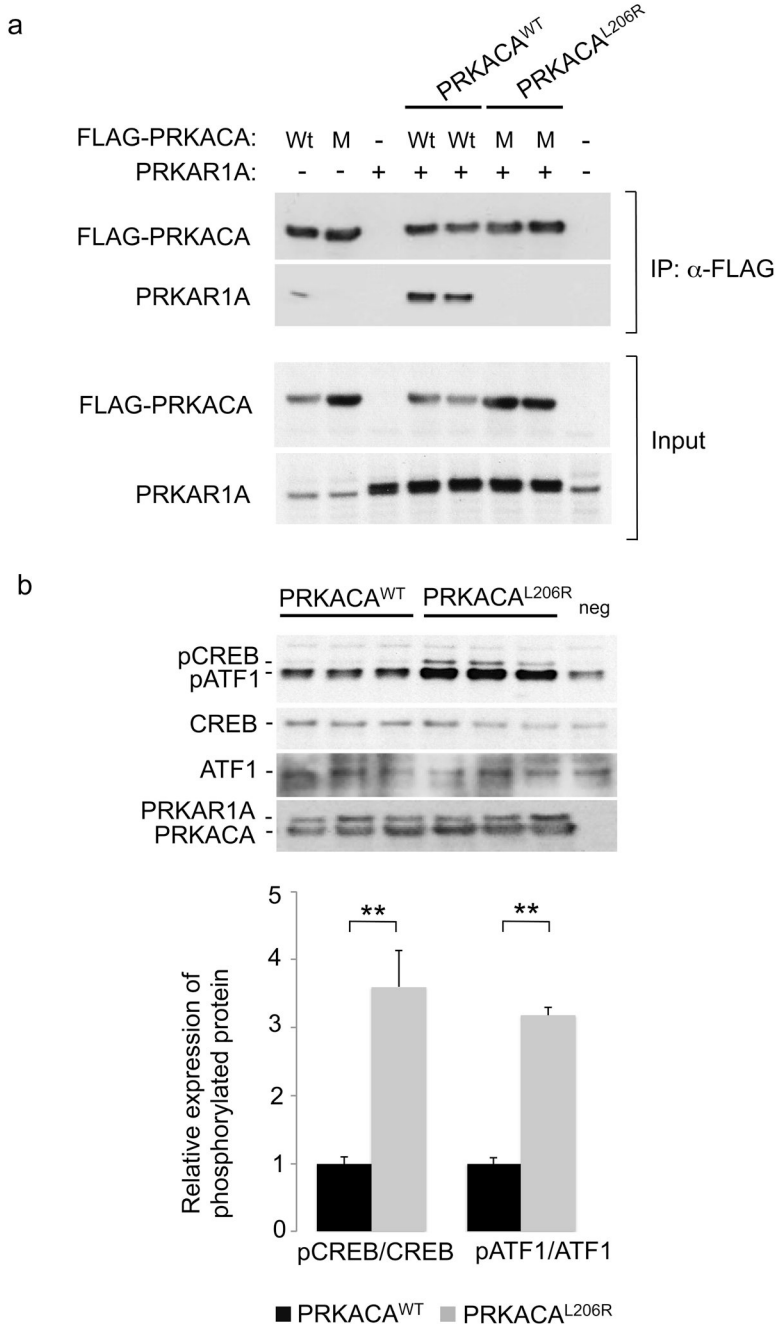

Figure 3.

PRKACA^{L206R} does not bind regulatory subunit and shows increased phosphorylation of CREB and ATF1. **(a)** FLAG-tagged constructs of wild type (Wt) or mutant (M) catalytic subunits (PRKACA^{WT} and PRKACA^{L206R}) and the regulatory subunit (PRKAR1A) were expressed in HEK293 cells in indicated combinations. Cell lysates were immunoprecipitated with anti-FLAG and the products of IP were analyzed by Western blotting with antibodies specific for FLAG and PRKAR1A. While IP of PRKACA^{WT} pulls down the regulatory subunit, IP of PRKACA^{L206R} does not. Duplicates shown are from independent

transfections. (**b**) Western blots with antibodies specific for CREB phosphorylated at Ser133 (pCREB) and ATF1 phosphorylated at Ser63 (pATF), CREB, ATF1, and FLAG in cells expressing FLAG-tagged PRKAR1A and either wildtype or mutant PRKACA(both tagged with FLAG). Representative results of triplicate experiments are shown. Bar graph shows results of quantitation (mean ± SEM; $n = 3$). Cells expressing $PRKACA^{L206R}$ have 3 to 4-fold higher levels of pCREB and pATF1 than cells expressing $PRKACA^{WT}$ (**P<0.05). neg, no transfection of PRKACA or PRKAR1A.